

Transporting Dispersed Cylindrical Granules: An Intelligent Strategy Inspired by an Elephant Trunk

Yuwen Zhao, Jie Zhang, Siyuan Zhang, Peng Zhang, Guixin Dong,* Jianing Wu,* and Jinxiu Zhang*

Manipulating granular materials is a crucial function of robotic grippers.

However, the existing approaches always suffer from low efficiency when dealing with large quantities of dispersed granules. To overcome this challenge, inspiration is drawn from an African elephant (*Loxodonta Africana*), which can employ both fingertip extensions on the trunk tip to efficiently grasp dispersed granular food all at once by mediating state transition of granules. Herein, this bio-inspired intelligent strategy is integrated into a soft pneumatic gripper for transporting dispersed granules. To evaluate the critical actuation pressures while grasping granules, a library is constructed experimentally, and the effects of the initial relative height and relative lifting speed on the grasping success rate are examined. It is indicated in the experimental results that this trunk-inspired robotic strategy leads to a success rate of over 90% and saves \approx 50% duration of manipulation compared to the individual gripping fashion. Herein, new insights may be offered in this study into a novel manipulation strategy for efficiently transporting dispersed granular materials.

1. Introduction

Manipulation by hand is a fundamental activity that humans learn from an early age.^[1] In industry, repetitive manipulation tasks

can be labor-intensive for humans. Consequently, the robotic grippers, which build interfaces between the robotic arm and the environment, have been developed to assist or even replace humans by continuously acquiring dexterous manipulation strategies.^[2] Currently, traditional rigid robotic grippers dominate in practical applications for their accurate power transmission, high load-bearing capacity, and precise position control.^[3] However, the rigid components of these grippers may be a stumbling block for compliant interaction with objects (especially fragile objects) and environments.^[4,5]

Soft grippers, in contrast, are characterized by inherent safety, and can actively or passively reconfigure their shape for adaptation of their elastic bodies to the objects they interact with.^[6] Existing soft grippers are capable of manipulating a wide range

of objects, including irregular-shaped,^[7,8] deformable,^[9] or fragile objects;^[10] however, most of these grippers are merely able to pick up the objects in an individual gripping fashion (Figure 1A), which may suffer from low efficiency when transporting large quantities of granular materials. Previous research has suggested three feasible strategies to handle a large concentration of granules (Figure 1B), which required specific scenarios to be created. The first approach is limited to gripping spherical granules, as it struggles to handle cylindrical granules due to their elongated shape (Figure 1Bi).^[11] The second approach proposes pre-stacking the granules in a container (Figure 1Bii); however, it is challenging to encapsulate the unconstrained granules.^[12,13] The third approach involves the use of an array of grippers on uniformly ordered granules (Figure 1Biii), which may exhibit low robustness for taking up disordered ones.^[14] Therefore, a practical technique for effectively handling scattered granules remained unexplored.

The difficulty of manipulating granular materials is intricately linked to their intrinsic physical properties. The granular aggregation, namely a large assembly of discrete grains,^[15] shares certain properties with both fluids and solids, distinct from individual grains featured in minute physical dimensions.^[16] The granular aggregation is commonly stable on the ground for the lowest gravitational energy of a monolayer of granules,^[17] and this aggregation exhibits different characteristics depending on the interparticle interactions when subjected to external stimuli and geometric boundaries.^[18,19] For instance, when the

Y. Zhao, J. Zhang, S. Zhang, J. Wu, J. Zhang
 School of Aeronautics and Astronautics
 Shenzhen Campus of Sun Yat-sen University
 Shenzhen 518107, P. R. China
 E-mail: wujn27@mail.sysu.edu.cn; zhangjinxiu@sysu.edu.cn
 P. Zhang, G. Dong
 Qingyuan Chimelong National Ex-situ Conservation Base of World
 Endangered Flora and Fauna
 Guangdong Chimelong group Co. Ltd.
 Guangzhou 511400, P. R. China
 E-mail: dgx@chimelong.com

J. Wu
 School of Advanced Manufacturing
 Shenzhen Campus of Sun Yat-sen University
 Shenzhen 518107, P. R. China

 The ORCID identification number(s) for the author(s) of this article can be found under <https://doi.org/10.1002/aisy.202300182>.

© 2023 The Authors. Advanced Intelligent Systems published by Wiley-VCH GmbH. This is an open access article under the terms of the Creative Commons Attribution License, which permits use, distribution and reproduction in any medium, provided the original work is properly cited.

DOI: [10.1002/aisy.202300182](https://doi.org/10.1002/aisy.202300182)

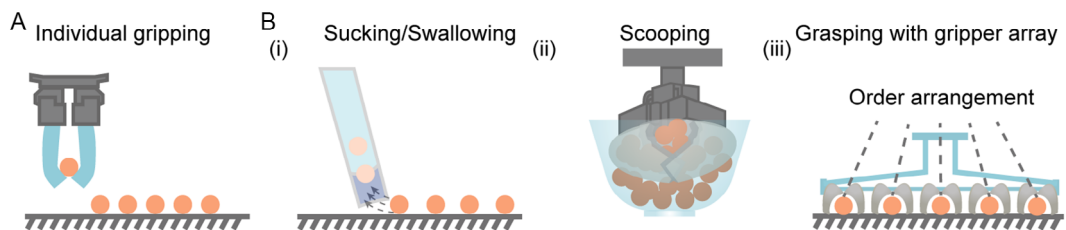


Figure 1. Traditional strategies of transporting granular materials. A) Gripping the objects in an individual grasping fashion. B) Previous strategies that can transport multiple granules at once: i) a gripper swallows spherical granules;^[11] ii) a gripper consisting of wide petals is used to scoop the pre-piled granules;^[12,13] and iii) an array of grippers grasp granules distributed uniformly.^[14]

granules are discrete with no or partial interactions among them, the aggregation exhibits a liquid-like characteristic with compliance to the deformable boundaries, while this property can be switched into a solid-like feature with high stiffness if all particles are interconnected under the boundaries and external forces.^[20] Moreover, the solid-like state is also prone to be broken when any infinitesimal particle displacement occurs, known as metastability.^[21] The nature of state transition makes the granules hard to be transported efficiently by robotic techniques.

Grasping is a fundamental function of animals appendages;^[22,23] therefore, physiological behavior of animals may inspire next-generation robotic grippers.^[24–27] A wild African elephant

(*Loxodonta Africana*) is a voracious eater whose daily dietary consumption approximately reaches 200 kg.^[28] In these food, the granular objects, such as grass, peanuts, and pellet feed, account for 10% of the total weight, estimated to be 69 000 pellets. Ingesting these types of food would cost 38 h at least on daily consumption of granular food provided that the elephant merely picks up one particle during each fetch that lasts 2 s. Notably, the elephant manipulates its trunk tip to grasp the granular food at once to improve the feeding efficiency (**Figure 2B**), resulting in a feeding rate of $\approx 180 \text{ g min}^{-1}$ and reducing the feeding time to 18 h d $^{-1}$.^[28,29]

Herein, inspired by the feeding behavior of an African elephant, we integrated an intelligent strategy into a soft gripper

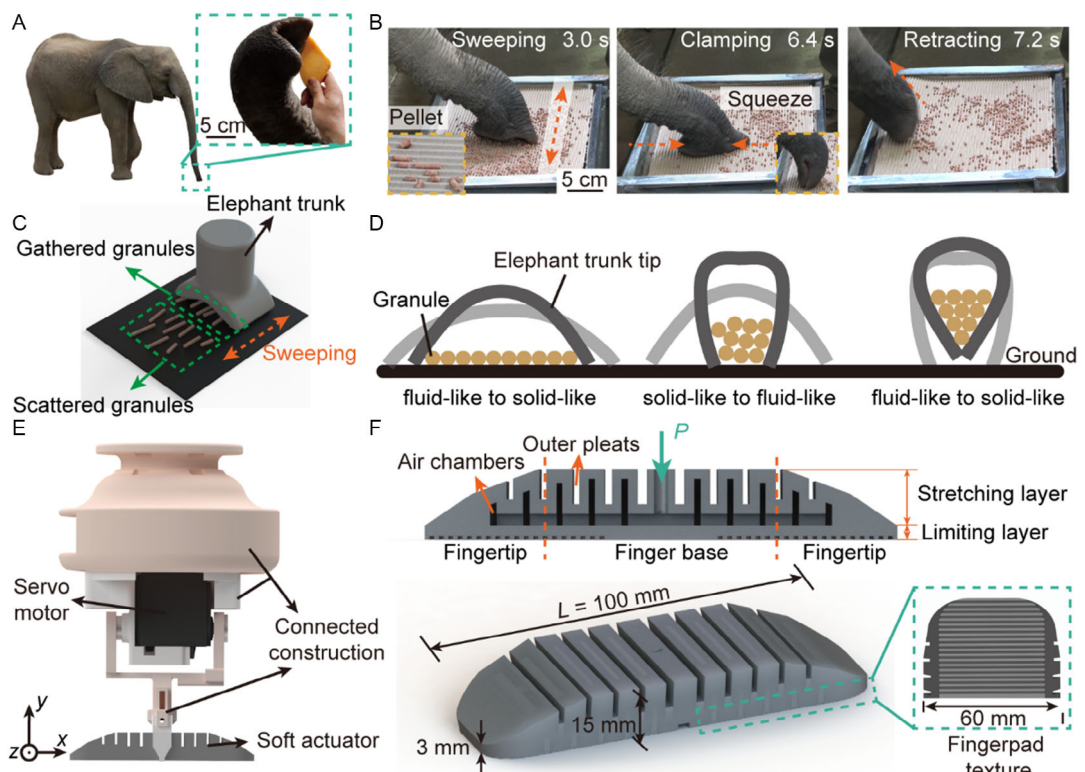


Figure 2. Transport strategy of an African elephant trunk tip for feeding on granular food. A) Photograph of an African elephant (left) and the fingertip extensions of its trunk (right). B) Key events of a living elephant trunk to transport the scattered granules. The arrowed dashed lines indicate movements of trunk body (at 3.0 and 7.2 s) and trunk tip (at 6.4 s). C) Schematics of sweeping to gather granules. D) State transition of the granular aggregation while clamping. E) A soft gripper inspired by an elephant trunk tip. A right-handed coordinate $x-y-z$ is established with the x axis aligning along the long way of the gripper, and the y axis going about the axis of the connected construction. F) Design of the soft pneumatic actuator (SPA).

(Figure 2E) for transporting scattered granules. Unlike the traditional strategy to grasp scattered granules individually, our gripper utilizing bio-inspired strategy can transport all dispersed granules in one grasp with a high success rate. We demonstrated the vast potential for utilizing this biological intelligence in the transportation of dispersed granules.

2. Results and Discussion

2.1. Granule Grasping by an Elephant Trunk Tip

We filmed the feeding behavior of a 13 year-old male African elephant (*Loxodonta Africana*). The elephant could employ the fingertip extensions at distal end of its trunk to grasp multiple scattered granules at once during feeding (Figure 2A). As illustrated in Figure 2B (Video S1, Supporting Information), the elephant initiates the feeding process by utilizing the lateral side of its trunk tip to sweep the board, enabling it to gather granules within 3 s (Figure 2C). Subsequently, the trunk tip attaches firmly to the board and squeezes the gathered granules from both sides to clamp them, and ultimately retracting its trunk tip to feed itself on the granules. During the clamping of granules, the granular aggregation undergoes multiple state transitions, as illustrated in Figure 2D. The firm contact between the tip and the board prevents any leakage of granules, while the squeezing action causes the granular aggregation to undergo alternating transitions between solid and fluid states (Figure 2D). This strategy, which builds a scenario capable of highly adapting to physical nature of granules, allows the elephant to capture a larger number of granules in each fetch, potentially enhancing the feeding efficiency. This strategy has the potential to inspire a novel robotic gripping mechanism, so we aim to establish a connection between the animal physiology and robotic gripper with optimal control framework in the following sections.

2.2. Trunk-Tip-Inspired Soft Gripper

Here, we developed a soft gripper to testify this bio-inspired transport strategy. As depicted in Figure 2E, the gripper is composed of two parts according to their distinct functions. The upper part is composed of a servo motor and a connected

construction that enables switching between sweeping and clamping operations. Then, a soft pneumatic actuator (SPA) is installed on the gripper for interacting with the target object. As shown in Figure 2F, the SPA consists of a wrinkled stretching layer and a flat limiting layer. Upon application of pressure P from the air inlet, the stretching layer, featured in both air chambers and outer pleats, expands and bends toward the limiting layer, which exhibits higher stiffness.^[30] In conjunction with the stretching and limiting layers, the SPA forms a two-fingered profile with a length of $L = 100$ mm, structurally analogous to an elephant trunk tip. Compared to the traditional two-fingered profile, this SPA is characterized by a one-body design paradigm that results in lengthy fingers and wider finger pads, facilitating sweeping of scattered granules and the grasping of gathered cylinders.^[13] The fingertips with a descending thickness from 15 to 3 mm ensure consistent contact with granules while manipulating, which enhances pinching of small targets.^[31] Moreover, they form a tight seal against the ground, preventing any leakage of cylinders even under large bending deformation. The finger pads are coated in a wrinkled texture to enhance grasping friction. We then fabricated the SPA in the way of soft lithography using silicone elastomer (Dragon Skin 30).^[32] The procedures for fabrication are illustrated in Figure S2, Supporting Information (Experimental Section).

2.3. State Transition of Granules Regulated by the Gripper

We then emulated the grasping behavior of the elephant by this soft gripper. The sweeping action is performed by tilting the SPA using a servo motor from its original vertical position along the x -axis of the gripper, and then coordinating with a robotic arm to move the tilted SPA for particle collection. Next, the SPA rights back vertically to perform clamping. Based on the primary mechanism that causes a change in the state of the granules, the gripping process can be divided into two stages, namely the geometry actuation (GA) stage and the force actuation (FA) stage, as depicted in Figure 3. Specifically, we first pressurized the SPA in the GA stage to decrease the fingertip distance D with the grasping force F remaining approximately constant at a low value. The fingertips with decreasing distance can squeeze the fluid-like granules into a compact state. When the SPA is inflated

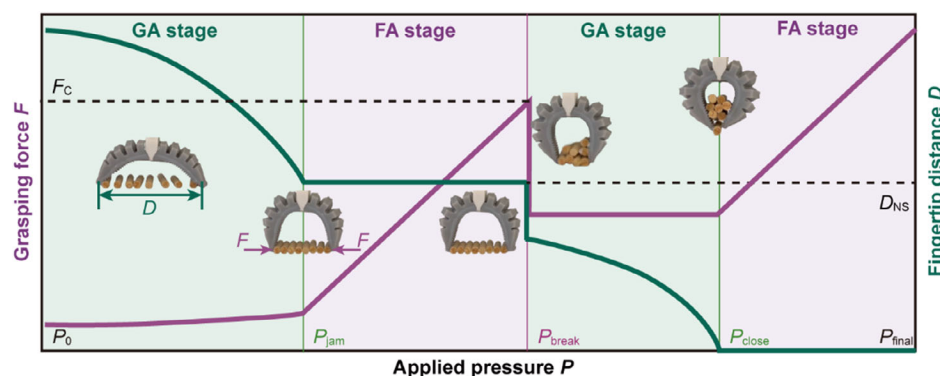


Figure 3. Phase-related operating mechanism of the SPA. Based on the primary mechanism that induces a change in the state of the granules, the gripping process can be categorized into two stages, namely the geometry actuation (GA) stage and the force actuation (FA) stage. Sudden drops of grasping force and fingertip distance during gripping possibly result at the pressure of P_{break} from the critical force exerted by the SPA on the granules.

with an air pressure of P_{jam} , the fingertip distance declines to D_{NS} , forming a solid granule chain with no clearances. Further pressurization results in the transition of the actuation stage from GA stage to FA stage. During FA stage, the fingertip distance remains unchanged, while the grasping force augments with the increasing applied pressure. Until the applied pressure reaches a critical pressure P_{break} , the granule chain can be broken under a grasping force F_{C} . As the chain of granules collapses, the SPA reverts to the GA stage and the energy that was stored in it is quickly released. This causes the SPA to bend rapidly and grasp the granules exhibiting fluid-like physics. Continued inflation of the SPA enables the fingertips to fully close at a pressure of P_{close} . The SPA then enters the FA stage, producing an increased grasping force that ensures stable gripping for transport. Practically to accomplish a successful grasp, the SPA is required to generate a sufficient horizontal force that is validated correlated to the additional pressure ΔP (more details can be found in Supporting Information), which is proceeded in the following section.

We regulated the position of the SPA installed on a rigid robotic arm (Z-Arm 1832, Hitbot, China) at a relative height of $H_r = 0.3$ away from the platform, and set the relative lifting speed of the SPA as $v_r = 0.1 \text{ s}^{-1}$ (Figure 4A). This critical relative height ensured that the SPA did not contact the flat surface during the bending deformation and that the granules were within the reach of the SPA. Here, the relative height H_r and the relative speed v_r are defined as the ratio of the height of the SPA H to L and the lifting speed of the SPA v to L , respectively. We prepared diverse granules in varying granularities S , and defined the

grasping success rate $\eta = N_s/N$ to evaluate the grasping performance of the SPA, in which N_s and N represent the number of successfully grasped granules and the total number of granules, respectively (Figure 4B). The SPA might exhibit enhanced adaptability of grasping granules with either varying granularity and quantities through simply increasing the additional pressure.^[33,34] However, excessive additional pressures may result in two issues: burst failure of the SPA and energy overconsumption. Therefore, we suggested a decision-making approach that selects a minimum additional pressure to actuate the SPA for a secure grasp. Here, we considered a success rate of $\eta = 90\%$ as the benchmark to identify a successful grasp, and depicted the minimal additional pressure boundary that attains a 90% success rate with a yellow line in Figure 4C. We found that the minimal additional pressures above the benchmark vary with both the number of granules and the granularity. For example, for all granules in a relative size of $S_r = S/L = 0.05$, gripping $N = 13$ granules requires an additional pressure of $\Delta P = 50 \text{ kPa}$ at minimum. Comparatively, we should use merely $\Delta P = 10 \text{ kPa}$ to pick up the granules in a number of $N = 3$, which reduces the additional pressure by 4 times (Figure 4Ci). Likewise, when grasping granules in the same quantity of $N = 5$, an additional pressure $\Delta P = 20 \text{ kPa}$ is sufficient to secure and grip the granules in a varied relative size S_r ranging from 0.04 to 0.06, while handling granules in a relative size of $S_r = 0.12$ requires $\Delta P = 60 \text{ kPa}$ (Figure 4Cii). To further reveal the relationship among the additional pressure threshold, the granularity, and the number of granules, we figured out a series of granule

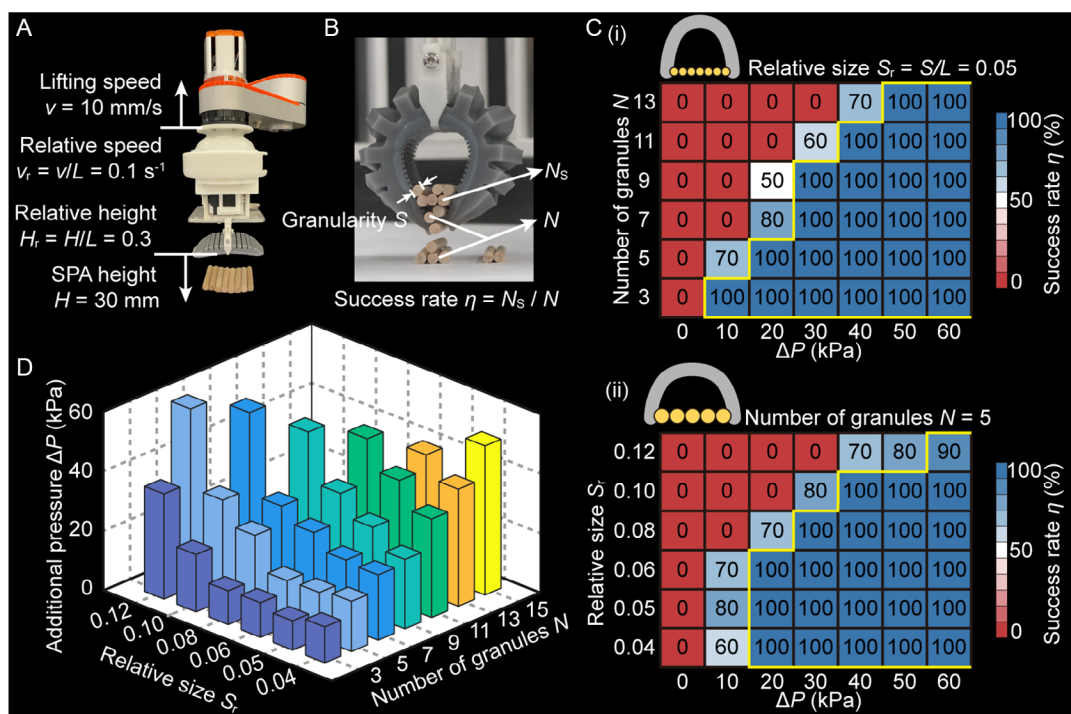


Figure 4. Critical applied pressures to actuate the SPA when grasping granules. A) The experimental setup for grasping granules. The SPA is initially located at a relative height of $H_r = H/L = 0.3 \text{ s}^{-1}$, and is lifted with a relative speed of $v_r = v/L = 0.1$ after being inflated. B) The definition of success rate η . N and N_s represent the total number of granules and the number of granules that are grasped up successfully, respectively. C) Map of the success rates of grasping granules i) in an identical relative size $S_r = 0.05$, and ii) with identical quantity $N = 5$. The yellow line illustrates the additional pressure boundary for a 90% success rate. D) The minimum additional pressure to grasp target granules at a threshold of a success rate of 90%.

configurations and introduced the SPA to take them up (Figure S4A, Supporting Information). We extracted the minimum additional pressures above the threshold in each case and illustrated them in Figure 4D. By categorizing the granule configurations into 7 groups according to the quantity N , the relation between the additional pressure ΔP and the relative size S_r can be fitted as Figure S4B, Supporting Information.

We then constructed a library based on these relations, which enables applied pressure regulation according to the size and quantity of target granules. For example, to grasp the granules characterized as $S_r = 0.07$ and $N = 7$, we should actuate the SPA to an additional pressure of $\Delta P = 29$ kPa; therefore, the corresponding applied pressure reaches $P = 88$ kPa. In the scenario of grasping an even number of granules, we can estimate the necessary additional pressure by averaging the pressures of the adjacent odd-numbered granules with the same size. This approximation method was confirmed by the experiments in Figure S4C, Supporting Information. For example, to grasp 8 granules in a relative size of 0.08, the additional pressure can be set to 44 kPa, which is the average of the additional pressures for 7 and 9 granules with a relative size of 0.08 (36 and 53 kPa, respectively). Thus, by using the quantity and granularity of the target granules as input, we can establish a method for controlling the applied pressure, enabling the SPA to grip granules with different sizes and quantities.

2.4. Grasping Performance

To explore the grasping performance of the transport strategy enabled by the bio-inspired soft gripper, we built a scenario for grasping dispersed granules as shown in Figure 5A.

An air pump equipped with a programmable logic controller (S7-200 SMART, Siemens, German) is employed to regulate the applied pressure for inflating the gripper. Additionally, we use a microcontroller (Arduino UNO, Arduino, Germany) to control a servo motor that makes the soft gripper tilt (Figure 5B). We prepared wooden granules with the relative size of $S_r = 0.12$, corresponding quantity is $N = 5$. As shown in Figure 5C, we first implemented the sweeping motion of the SPA by coordinating the robotic arm and the servo motor for gathering the scattered granules. Then, we tuned the SPA to a vertical position using the servo motor, and located the SPA to a relative height of $H_r = 0.25$. To determine the total applied pressure, we selected an additional pressure value of $\Delta P = 59$ kPa based on the library, and added this pressure to the critical jamming pressure, $P_{jam} = 50$ kPa, resulting in a total applied pressure of $P = 109$ kPa. Then, we adopted this applied pressure to actuate the SPA for grasping the gathered granules, and demonstrated that the success rate of grasping η reaches 100% (Figure 5Ci and Video S2, Supporting Information). We also analyzed the duration required for transporting these scattered granules. Our bio-inspired intelligent approach took around 24 s, which is only half of the time required for the traditional individual gripping method (as shown in Figure 5Cii and Video S2, Supporting Information). This highlights the high efficiency of our transportation strategy.

To further enhance the grasping performance of our gripper, we extracted two physical/kinematic parameters of the robotic system that may influence the grasping success rate, including the relative height H_r and the relative speed v_r . We first kept the relative speed unchanged as $v_r = 0.1 \text{ s}^{-1}$, and measured the variation of grasping success rate at the relative height H_r ranging from 0.15 to 0.3 (Figure 6A). We found that $H_r < 0.3$ benefits for

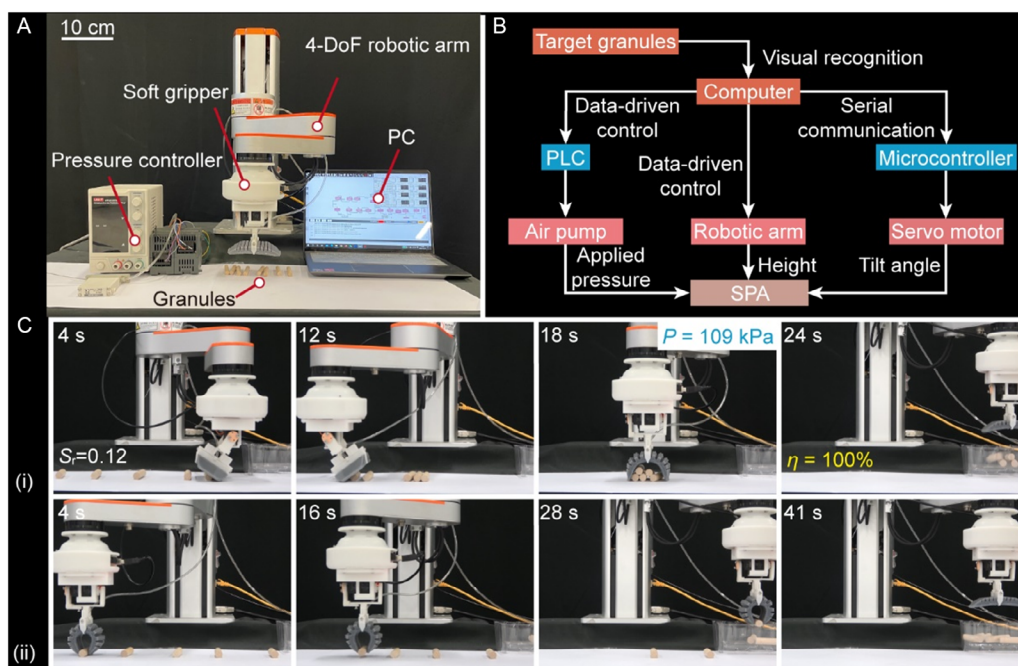


Figure 5. Performance of the soft gripper in transporting scattered granules. A) Experimental setup consisting of a 4-degree of freedom robotic arm, a pressure controller, a personal computer, and the soft gripper. B) The control system for the soft gripper. C) Comparison of the duration of the bio-inspired operation strategy i) with the individual gripping fashion ii) for grasping five granules in an average relative size of 0.12.

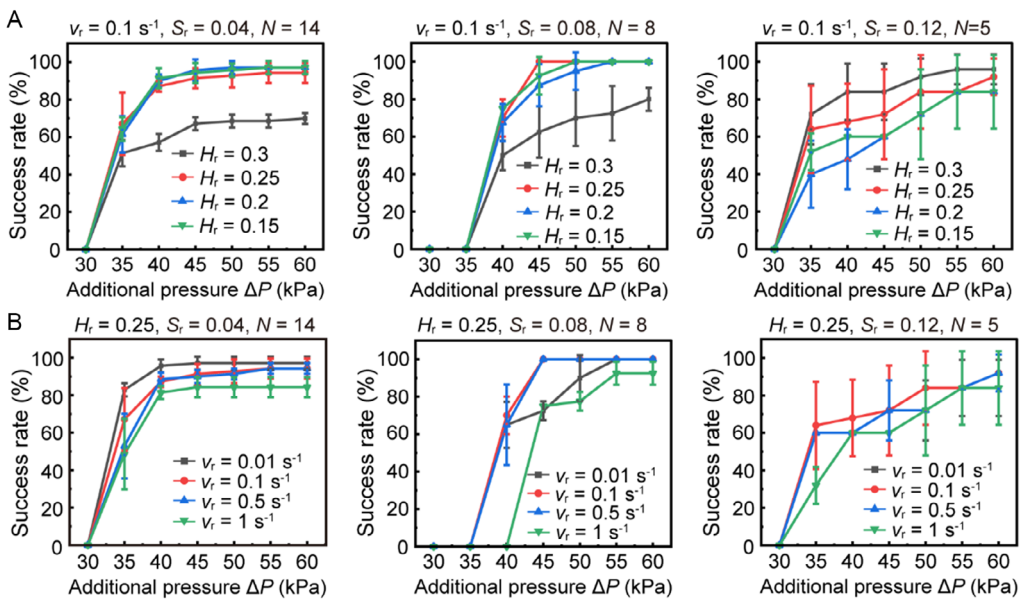


Figure 6. Effects of the initial relative height and relative lifting speed of the soft gripper on the grasping success rate. A) Comparison of gripper grasping performance in the relative height ranging from 0.15 to 0.3. B) Comparison of gripper grasping performance at a relative speed v_r between 0.01 and 1 s^{-1} .



Figure 7. Soft gripper inspired by the gripping fashion of an elephant trunk tip for transporting scattered granular food. A) Crispy bars. B) Finger cookies. C) Penne. D) Wafer rolls. i) Scattered granular food with varying granularities and quantities. ii) Edge detection of the granular food. iii) Snapshots of the transporting process.

grasping granules in a relative size of 0.04 and 0.08, which may be attributed to the fact that lowering the height may geometrically configure a secure contact between the gripper and platform, ensuring no leakage of granules during the process of grasping (Figure S5, Supporting Information). By contrast, when grasping granules with $S_r = 0.12$ using an additional pressure of $\Delta P = 50 \text{ kPa}$, the success rate can be significantly enhanced by grasping at $H_r = 0.3$ ($\eta = 92.0 \pm 9.8\%$), compared to applying the other relative heights ($\eta = 84.0 \pm 19.6\%$ at $H_r = 0.25$, $\eta = 72.0 \pm 24.0\%$ at $H_r = 0.2$ and 0.15). Then, we kept the relative height as a constant of $H_r = 0.25$ to evaluate the effect of the relative speed v_r ranging from 0.01 to 1 s^{-1} on the grasping performance (Figure 6B). We found that the relative speed of $v_r = 0.5 \text{ s}^{-1}$ is applicable for grasping all these granules. Therefore, we could adopt customized operation strategies for the robotic arm according to the granularity.

2.5. Application Demonstration

We expanded the possible uses of our soft gripper in the food industry by correlating physical parameters, including applied pressure, initial relative height, and relative lifting speed, on grasping success rate. This includes handling delicate granular foods like crispy bars, finger cookies, penne, and wafer rolls as demonstrated in Video S3 and Supporting Information. To grasp these granular foods, we first extracted their relative size and quantity by the image detection techniques (more details in Experimental Section). Based on this information, we could figure out the critical applied pressure to inflate the gripper with the logic flow shown in Figure S6, Supporting Information. The experimental results reveal that the data-driven soft gripper can transport the dispersed granular food with high efficacy in both duration (24 s) and success rate (average over 90%, 5 trials), as demonstrated in Figure 7. This indicates that the robot integrating with the bio-inspired intelligent strategy has a favorable ability to transport the dispersed granular food in altered granularity and quantity.

3. Conclusion

In this study, we uncovered an intelligent strategy employed by an African elephant to efficiently transport granular food using its trunk tip, which can mediate the transition of granules between solid and liquid states. We then integrated this strategy into our soft gripper for efficient granule transportation. To achieve accurate actuation of the gripper, we constructed a library to determine the critical applied pressure for grasping granules. The experimental results demonstrate that this bio-inspired transport strategy exhibits a success rate of over 90% in grasping granules and the time consumption can be reduced by almost half compared to the individual gripping fashion, making it a promising technique for manipulating granules in production lines. Our study specifically addresses the task of grasping cylindrical granules. However, handling irregularly shaped granules may pose difficulties for the current structure. Hence, future studies will investigate the incorporation of suction methods with grasping to collect granules of diverse shapes, similar to how an elephant gathers various granules.^[29]

4. Experimental Section

Fabrication of the SPA: The molds for casting the SPA were fabricated with resin based on stereo lithography apparatus (SLA) 3D-printing technology. Then we sprayed the release agent (Easy Release 200, Smooth-on Inc., USA) onto the mold surfaces and dehydrated them in the lab environment (25 °C, 1 atm) for 5 min. The two precursors (Dragon Skin 30 Part A and Part B, Smooth-on Inc., USA) were measured in a ratio of 1:1 by weight and mixed for 3 min. After de-bubbling for 10 min by using a vacuum tank, we poured the mixture into mold 2 and mold 3, and inserted mold 1 into mold 2. After 4 h at ambient temperature for curing the limiting and stretching layers, we peeled off the stretching layer, and added 10 g of the mixture onto the limiting layer for bonding the two layers. When the silicone rubber solidified, we trimmed the SPA and inserted a tube into the airway entrance of the SPA, and then inflated it to check the air tightness.

Evaluation of success rate: For the SPA grasping experiment (Figure 4C,D, 6 and 7), we attempted to grasping the target granules five times for each case, and recorded the mean value and standard deviation of the success rate. For the experiment shown in Figure 5C, the sweeping speed and lifting speed were both set to 50 mm s^{-1} , and the relative height was 0.25. The time reserved for grasping was set to 3 s. Before the sweeping operation shown in Figure 5Ci, the gripper first rotated 90° clockwise around the y-axis, and the SPA tilted to 30° from the vertical direction. Thereafter, the SPA descended to the flat surface, and the sweeping operation started.

Visual recognition module: To accurately grasp of scattered granular food, we not only extracted the image edge but calculated the applied pressure based on the library (Figure S6, Supporting Information). Specifically, we first captured photos of the scattered granules with a camera (EOS 6D Mark II, Canon, Japan), and then binarized and refined the image by Gaussian filtering in MATLAB R2020b. We then extracted their edges with Canny operator, and further refined the binary image by using morphological operation to eliminate the interference of the background and the grain surface texture.^[35] To count the number of granules and calculate the granularity, we labeled the center of each connected component in the binary image in a sequence, and calculated the contour size of each connected component from the pixel points.

Supporting Information

Supporting Information is available from the Wiley Online Library or from the author.

Acknowledgements

Y.Z. and J.Z. contributed equally to this work. The authors would like to express our sincere gratitude to Xurong Ma and Ruotong Sun for their valuable contributions to this study. This work was supported by the National Natural Science Foundation of China (Grant nos. 52275298 and 51905556), and Shenzhen Science and Technology Program (Grant nos. GXWD2021B03 and 20220817165030002).

Conflict of Interest

The authors declare no conflict of interest.

Author Contributions

J.W., and J.Z.: conceived the concept; Y.Z., S.Z., and P.Z.: carried out experiments and data processing; Y.Z., J.Z., J.W., and J.Z.: analyzed the data and interpreted the results; G.D., J.W., and J.Z.: directed the project. All authors commented on the article.

Data Availability Statement

The data that support the findings of this study are available in the supplementary material of this article.

Keywords

elephant trunk tip, granular materials, soft gripper, transport strategy

Received: April 13, 2023

Revised: May 24, 2023

Published online:

- [1] A. Billard, D. Kragic, *Science* **2019**, *364*, eaat8414.
- [2] R. M. Murray, Z. Li, S. S. Sastry, *A Mathematical Introduction to Robotic Manipulation*, CRC Press, Boca Raton, **2017**.
- [3] L. Zhou, L. Ren, Y. Chen, S. Niu, Z. Han, L. Ren, *Adv. Sci.* **2021**, *8*, 2002017.
- [4] J. Shintake, V. Cacucciolo, D. Floreano, H. Shea, *Adv. Mater.* **2018**, *30*, 1707035.
- [5] S. Chen, Y. Pang, H. Yuan, X. Tan, C. Cao, *Adv. Mater. Technol.* **2020**, *5*, 1901075.
- [6] H. Wang, M. Totaro, L. Beccai, *Adv. Sci.* **2018**, *5*, 1800541.
- [7] Z. Wang, K. Or, S. Hirai, *Rob. Auton. Syst.* **2020**, *125*, 103427.
- [8] W. Kim, J. Eom, K.-J. Cho, *Adv. Intell. Sys.* **2022**, *4*, 2100176.
- [9] Z. Zhang, X. Ni, H. Wu, M. Sun, G. Bao, H. Wu, S. Jiang, *Soft Rob.* **2022**, *9*, 57.
- [10] N. R. Sinatra, C. B. Teeple, D. M. Vogt, K. K. Parker, D. F. Gruber, R. J. Wood, *Sci. Rob.* **2019**, *4*, eaax5425.
- [11] D. Sui, Y. Zhu, S. Zhao, T. Wang, S. K. Agrawal, H. Zhang, J. Zhao, *Soft Rob.* **2022**, *9*, 36.
- [12] Y. Kuriyama, Y. Okino, Z. Wang, S. Hirai, in *2019 2nd IEEE Inter. Conf. on Soft Robotics (RoboSoft)*, IEEE, Seoul, Korea (South), **2019**, pp. 114–119.
- [13] S. Jain, S. Dontu, J. E. M. Teoh, P. Valdivia, Y. Alvarado, *Soft Rob.* **2023**, *10*, <https://doi.org/10.1089/soro.2021.0225>.
- [14] Y. Yang, K. Vella, D. P. Holmes, *Sci. Rob.* **2021**, *6*, eabd6426.
- [15] H. M. Jaeger, S. R. Nagel, R. P. Behringer, *Rev. Mod. Phys.* **1996**, *68*, 1259.
- [16] H. Deresiewicz, in *Advances in Applied Mechanics* (Eds.: H. L. Dryden, T. von Kármán), Elsevier, Amsterdam **1958**, pp. 233–306.
- [17] P. G. de Gennes, *Rev. Mod. Phys.* **1999**, *71*, S374.
- [18] S. Eristoff, S. Y. Kim, L. Sanchez-Botero, T. Buckner, O. D. Yirmibeşoğlu, R. Kramer-Bottiglio, *Adv. Mater.* **2022**, *34*, 2109617.
- [19] K. Desmond, S. V. Franklin, *Phys. Rev. E* **2006**, *73*, 031306.
- [20] M. Z. Miskin, H. M. Jaeger, *Nat. Mater.* **2013**, *12*, 326.
- [21] R. P. Behringer, B. Chakraborty, *Rep. Prog. Phys.* **2019**, *82*, 012601.
- [22] J. K. A. Langowski, P. Sharma, A. L. Shoushtari, *Sci. Rob.* **2020**, *5*, eabd9120.
- [23] K. Goldberg, *Sci. Rob.* **2021**, *6*, eabi9225.
- [24] R. Pfeifer, M. Lungarella, F. Iida, *Commun. ACM* **2012**, *55*, 76.
- [25] X. Le, W. Lu, J. Zhang, T. Chen, *Adv. Sci.* **2019**, *6*, 1801584.
- [26] C. Yoon, *Nano Convergence* **2019**, *6*, 20.
- [27] S. Wang, Z. Xie, F. Yuan, L. Li, Y. Liu, T. Wang, L. Wen, *Chin. Sci. Bull.* **2022**, *67*, 959.
- [28] J. Wu, Y. Zhao, Y. Zhang, D. Shumate, S. Braccini Slade, S. V. Franklin, D. L. Hu, *J. R. Soc. Interface* **2018**, *15*, 20180377.
- [29] A. K. Schulz, J. Ning Wu, S. Y. S. Ha, G. Kim, S. Braccini Slade, S. Rivera, J. S. Reidenberg, D. L. Hu, *J. R. Soc. Interface* **2021**, *18*, 20210215.
- [30] B. Mosadegh, P. Polygerinos, C. Keplinger, S. Wennstedt, R. F. Shepherd, U. Gupta, J. Shim, K. Bertoldi, C. J. Walsh, G. M. Whitesides, *Adv. Funct. Mater.* **2014**, *24*, 2163.
- [31] Y. Cui, X.-J. Liu, X. Dong, J. Zhou, H. Zhao, *IEEE Trans. Rob.* **2021**, *37*, 1604.
- [32] R. F. Shepherd, F. Ilievski, W. Choi, S. A. Morin, A. A. Stokes, A. D. Mazzeo, X. Chen, M. Wang, G. M. Whitesides, *Proc. Natl. Acad. Sci.* **2011**, *108*, 20400.
- [33] S. M. Mirvakili, D. Sim, I. W. Hunter, R. Langer, *Sci. Rob.* **2020**, *5*, eaaz4239.
- [34] Y.-F. Zhang, C. J.-X. Ng, Z. Chen, W. Zhang, S. Panjwani, K. Kowsari, H. Y. Yang, Q. Ge, *Adv. Mater. Technol.* **2019**, *4*, 1900427.
- [35] N. Miura, A. Nagasaka, T. Miyatake, *IEICE Trans. Inf. Syst.* **2007**, *90*, 1185.